

Article

Evaluation of a Compact Coaxial Underground Coal Gasification System Inside an Artificial Coal Seam

Fa-qiang Su ¹, Akihiro Hamanaka ² , Ken-ichi Itakura ³, Gota Deguchi ⁴, Wenyan Zhang ^{5,*} and Hua Nan ^{1,*}

¹ School of Energy Science and Engineering, Henan Polytechnic University, 2001 Century Avenue, Jiaozuo 454-003, China; sfqmuroran@gmail.com

² Department of Earth Resources Engineering, Kyushu University, Motooka 744, Nishi-ku, Fukuoka 819-0395, Japan; hamanaka@mine.kyushu-u.ac.jp

³ Graduate School of Engineering, Muroran Institute of Technology, 27-1 Mizumoto, Muroran 050-8585, Japan; itakura@mmm.muroran-it.ac.jp

⁴ Underground Resources Innovation Network, Non-Profit Organization (NPO), Higashi-ku, Sapporo 007-0847, Japan; gota@mue.biglobe.ne.jp

⁵ School of Materials Science and Engineering, Henan Polytechnic University, 2001 Century Avenue, Jiaozuo 454-003, Henan, China

* Correspondence: zhangwy@hpu.edu.cn (W.Z.); nanhua@hpu.edu.cn (H.N.)

Received: 10 March 2018; Accepted: 8 April 2018; Published: 11 April 2018



Abstract: The Underground Coal Gasification (UCG) system is a clean technology for obtaining energy from coal. The coaxial UCG system is supposed to be compact and flexible in order to adapt to complicated geological conditions caused by the existence of faults and folds in the ground. In this study, the application of a coaxial UCG system with a horizontal well is discussed, by means of an ex situ model UCG experiment in a large-scale simulated coal seam with dimensions of 550 × 600 × 2740 mm. A horizontal well with a 45-mm diameter and a 2600-mm length was used as an injection/production well. During the experiment, changes in temperature field and product gas compositions were observed when changing the outlet position of the injection pipe. It was found that the UCG reactor is unstable and expands continuously due to fracturing activity caused by coal crack initiation and extension under the influence of thermal stress. Therefore, acoustic emission (AE) is considered an effective tool to monitor fracturing activities and visualize the gasification zone of coal. The results gathered from monitoring of AEs agree with the measured data of temperatures; the source location of AE was detected around the region where temperature increased. The average calorific value of the produced gas was 6.85 MJ/Nm³, and the gasification efficiency, defined as the conversion efficiency of the gasified coal to syngas, was 65.43%, in the whole experimental process. The study results suggest that the recovered coal energy from a coaxial UCG system is comparable to that of a conventional UCG system. Therefore, a coaxial UCG system may be a feasible option to utilize abandoned underground coal resources without mining.

Keywords: acoustic emission (AE); underground coal gasification (UCG); coaxial UCG model; energy recovery

1. Introduction

Underground Coal Gasification (UCG) can exploit the energy stored in underground coal efficiently and with fewer environmental impacts. Valuable gas products can be obtained by gasifying coal in situ with a UCG operation [1–14]. The general UCG system, comprising of an injection well and a production well at the surface, is shown in Figure 1, in which both wells are connected by a

linking hole within the coal seam [15,16]. During the process of gasification, the gasification area is gradually enlarged along the linking hole. The product gases can be obtained, as they are useful in the creation of many products, such as chemical feed stocks, liquid fuels, hydrogen, synthetic gas, and the generation of electric power [17–22]. Recently, UCG technology has attracted greater attention as an alternative to conventional mining methods, especially when exploiting coal resources located deep underground or exploiting low quality coal resources with high ash and high sulfur. Gasification provides the technological basis for theoretical and experimental research of pollution control, specifically, the emissions of sulfur, nitrous oxides, and mercury, which is useful for the elimination of ash after coal burning. An alternative UCG system must be developed in Japan because its geological conditions are complicated by the existence of faults and inclined coal seams. Given this background, we are developing a coaxial UCG system that is compact, safe, and highly efficient, as shown in Figure 2. Only well drilling and a double pipe were used in the coaxial UCG system. Gasification agents are injected from the inner pipe to expand the combustion zone. The production gas is recovered from the outer pipe. The designated inner (injection) pipe can be slid up and down to adjust the gas outlet position.

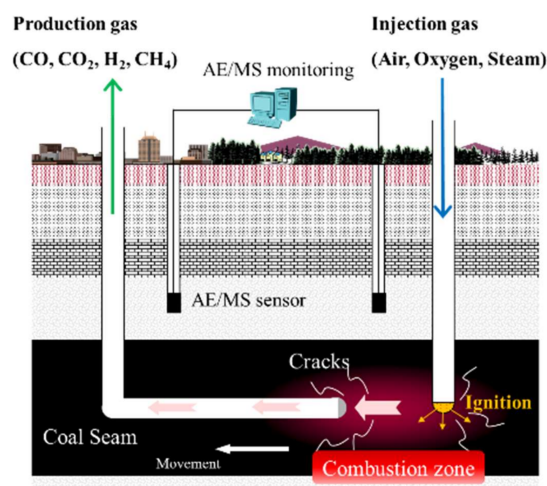


Figure 1. Traditional Underground Coal Gasification (UCG) process with monitoring system.

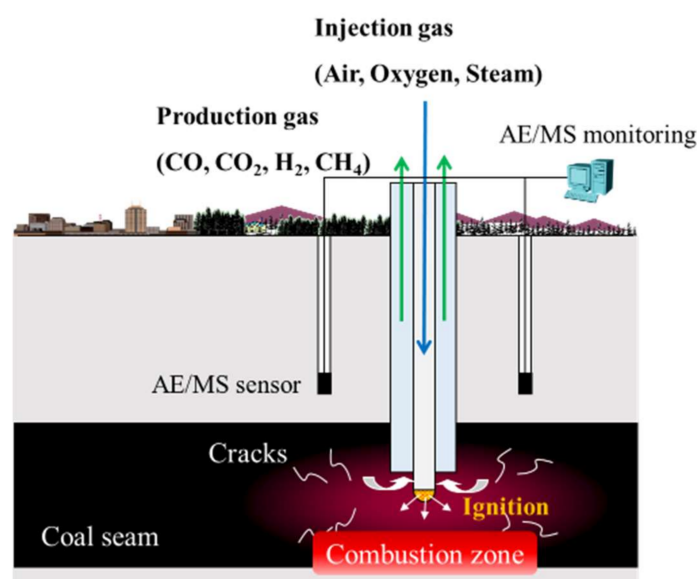


Figure 2. Coaxial UCG process with monitoring system.

However, associated environmental issues (such as gas leakage, groundwater pollution, and surface subsidence associated with cavity growth) [23–28], improperly executed operations, and gasification processes can restrict the applicability of UCG. Therefore, in order to ensure effective combustion and efficient gasification, the evaluation of the coal gasification cavity growth and precise control of the reactor are important. It was suggested that the gasification efficiency is directly affected by the enlargement of the oxidation surface around the gasification channel following crack initiation and development inside the coal seam. Several research activities were carried out to evaluate cavity growth and the velocity of the gasification flame, based on a mathematical model [8,29]. These research methods were effective in estimating the volume and progress of cavity growth and in creating the design of the UCG operation, however these methods were also needed to evaluate the cavity in real-time during the UCG operation, because it is sometimes difficult to predict the cavity in a coal seam precisely due to its heterogeneous characteristics. In order to evaluate fracturing activity around the combustion area, acoustic emission (AE) monitoring was applied in our previous research [30]. It has been proven that the AE technique has great potential for the measurement of fracture extension around the combustion reactor. In typical UCG, a geophone, a type of transducer with low frequency microseismicity, which is functionally similar to the AE accelerometer employed in this work, could be used to monitor fracturing occurring inside the gasifier. This technique makes it clear when and where microfailure phenomena occur. Until now, various UCG model experiments have been carried out to develop the coaxial UCG system [31–33]. However, the energy recovered from the coal is relatively low because the gasification area in a coaxial system is limited around a well. Therefore, an application of the coaxial UCG system with a horizontal well is discussed to improve the total efficiency of the gasification process in the study (Figure 3). The coaxial UCG system is expected to be used as a local energy source in small communities, as the cost of constructing drill holes and purchasing ground equipment is lower than those for the traditional UCG system that has a linking hole.

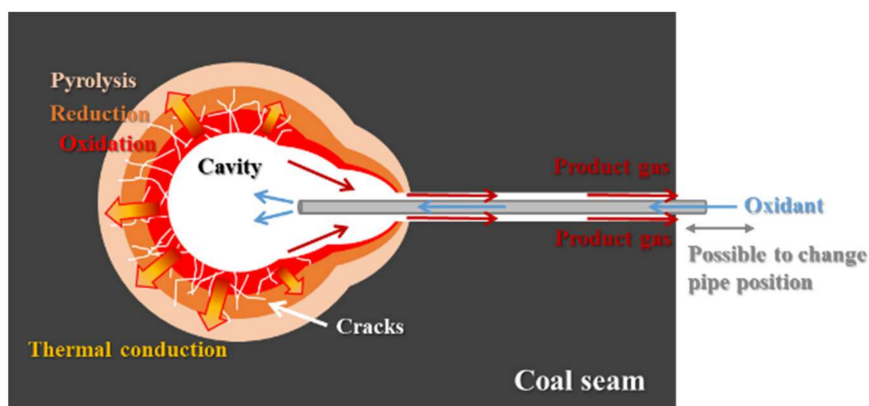


Figure 3. Coaxial UCG system with a horizontal well.

This paper presents *ex situ* experiments conducted with the coaxial type UCG model. In order to simulate UCG conditions with the coaxial-hole model in an artificial coal seam, the research team designed and established larger-scale UCG systems, which were different from the previous laboratory-scale model experiments [31–36]. We also estimated the energy recovery and gasification efficiency with a theoretical calculation, based on the measured product gases.

Results obtained from this experiment revealed that coal generated AEs with special AE activity patterns that were caused by thermal stress. The AE technique can visualize fracture extension around the combustion reactor. The results from gas energy recovery were evaluated with a stoichiometric method [36], based on the measured product gas compositions. After approximately 72 h of UCG operation in this experiment, product gas with an average calorific value of approximately 6.85 MJ/m³ was produced.

2. Material and Methods

Description of the Simulated UCG Gasifiers

The ex situ experiment described in this report was conducted in an artificial coal seam. Figure 4. presents the typical dimensions and structure of the UCG experimental system—the coaxial-hole model. A coaxial well was used as the ignition and production well and was prepared in the lower part of the simulated coal seam, 125 mm from the bottom of the seam, with 2600 mm length, and 45 mm diameter. The coaxial pipe line was equipped for gas injection and production. The outlet position of the gasification agents could be adjusted by controlled movement of the inner pipe. The coal seam was prepared as a rectangle with the external dimensions of 2.842 m (length) \times 0.600 m (width) \times 0.55 m (height).

The ultimate and proximate analysis result of the coal used in the experiment is shown in Table 1. The characteristics of the coal samples were low sulfur (0.07%) content and low ash content (4.30%), and were supplied by the Sanbi Mining Co., Ltd. (Mikasa, Japan). This coal is abundant in Hokkaido, Japan, and has the potential to provide high-calorie gas for power generation by UCG.

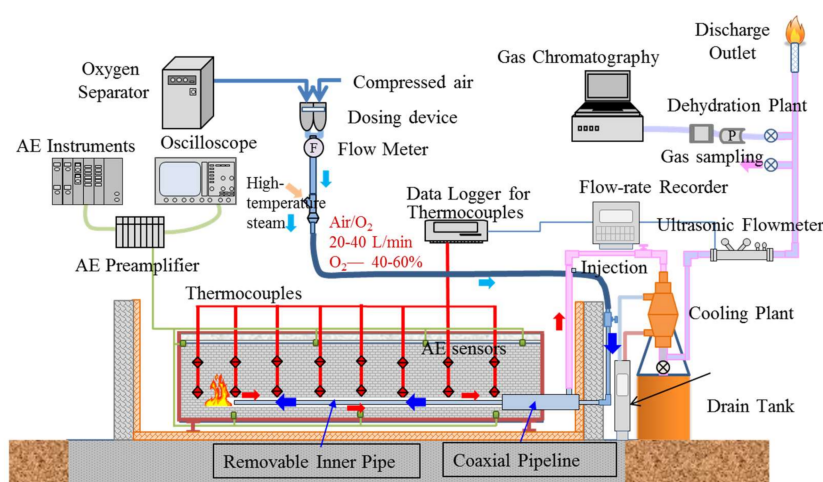


Figure 4. UCG experimental system, the coaxial-hole model.

Table 1. Proximate and ultimate analysis of coal samples.

| No. | Parameter | Sanbi Coal (Japan) |
|----------------------------------|-----------------|--------------------|
| Proximate analysis/(wt %) | | |
| 1 | Fixed moisture | 2.10 |
| 2 | Ash content | 4.30 |
| 3 | Volatile matter | 43.10 |
| 4 | Fixed carbon | 50.50 |
| 5 | Total sulfur | 0.07 |
| Ultimate analysis/(wt %) | | |
| 6 | Carbon | 78.40 |
| 7 | Hydrogen | 5.74 |
| 8 | Nitrogen | 1.44 |
| 9 | Oxygen | 9.94 |

Ignition is an important process, and is required to rise coal temperature in order to start the UCG process, since product gas could be generated due to the promotion of chemical reactions around the high temperature area. In this study, a laser ignition system, with oxygen supply, was adopted to

easily, safely, and quickly ignite the coal (Figure 5). We used semiconductor laser equipment (M710A45; Omron Laserfront Inc., Kanagawa, Japan), which had a laser emission wavelength of 808 nm and rated output of 45 W. The ignition process was achieved by emitting the laser to the bottom of the coaxial well from a distance of 150 mm with available oxygen supply.

After igniting the coal, a gas mixture containing air and oxygen was injected continuously at 35 L/min. Meanwhile, the oxygen concentration was kept at a stable 50%. During the experiment, the temperature, flow rate, and the composition of product gas were measured. Temperature was monitored using type K thermocouples (SUS310S; Chino Corp., Tokyo, Japan) and a data logger (GL220; GRAPHTEC Corp., Tokyo, Japan). Figure 6 shows the distributions of sensors. The flow rate of the produced gas was monitored using an ultrasonic flowmeter (DigitalFlow™ GM868). The product gas compositions (O_2 , N_2 , CO_2 , H_2 , CO , CH_4 , C_2H_4 , C_2H_6 , C_3H_6 , and C_3H_8) were measured every hour using a gas chromatograph (Micro GC 3000A; Inficon Co., Ltd., Yokohama, Japan). The AE events from sensors mounted inside the coal seam were recorded using a data logger (GL900; Graphtec Corp., Yokohama, Japan). The AE waveforms were detected by sensors and recorded in the multi-recorder oscilloscope (GR-7000; Keyence Co., Osaka, Japan) with a sampling time of 10 μ s. The temperature profiles recorded by the thermocouples were crucial for controlling process development and cavity growth.

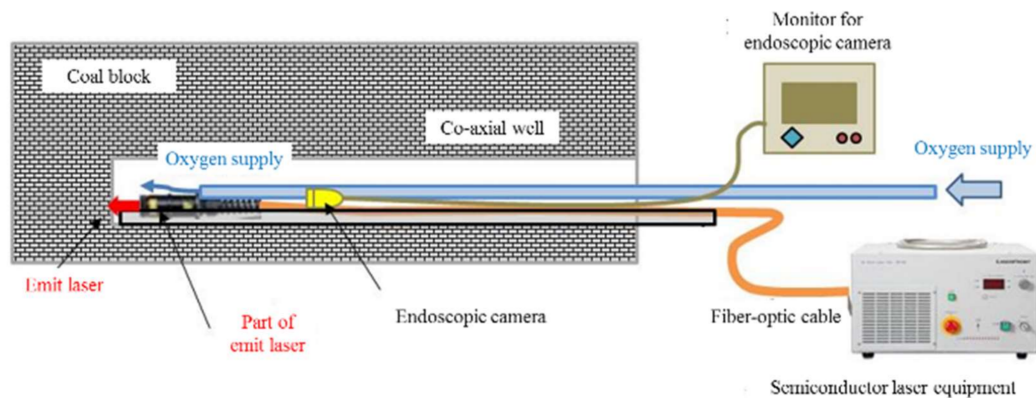


Figure 5. Laser ignition system.

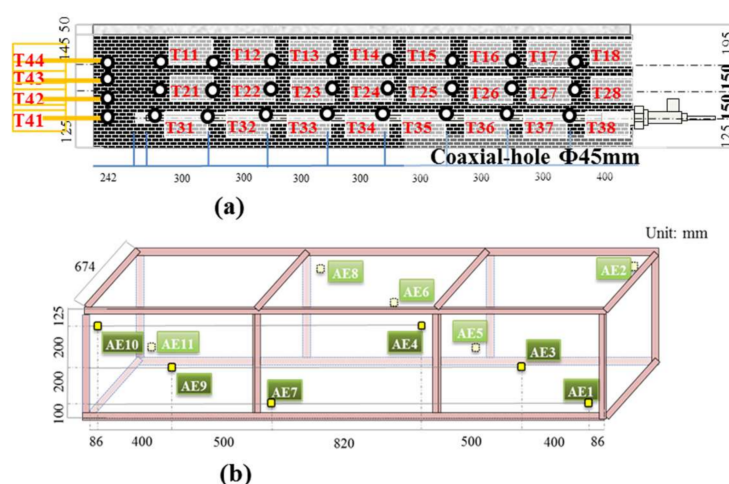


Figure 6. Deployments of thermocouples and acoustic emission (AE) sensors in the experimental model. (a) Thermocouples arrangement; (b) AE sensors arrangement.

Additionally, the position of the injection pipe was changed periodically by 300 mm toward the inlet of oxidant in order to move the gasification area when the gasification reactions were not active.

The gasification period was 72 h because the experiment was stopped prematurely due to trouble with the experiment equipment. After this process, a grouting material made by Portland cement and gypsum was filled into the cavity after gasification, to measure and calculate the cross-sectional area of the combustion zone.

3. Results and Discussion

3.1. Gasification Zone Evolution

3.1.1. Temperature Distribution

Figure 7a–d shows the results of temperature profiles during the gasification process. The highest local temperature recorded during the experiment was approximately 1400 °C (T15-16, located in the vicinity of the roof part of the reactor). After the beginning, the temperatures recorded by T11, T12, and T13, rose gradually and reached a peak. It could be inferred that the coal was ignited successfully at the bottom of coaxial hole. The injection pipe was moved outward a certain distance (approximately 30 mm) at the operation times of 23.7 h, 38.1 h, 47.0 h, 63.3 h, and 73.6 h. The temperatures of the thermocouples, which were located just above the coaxial hole, increased sequentially, along with adjustment of the oxygen outlet position, which depicted propagation of the combustion zone as well as the coaxial hole ignition position. As shown in Figure 7a, although the highest temperature around T14 and T15 (located in middle region) was recorded at approximately 800 °C, the temperature of the other thermocouples was still increased and reached over 1000 °C, showing that the gasification zone was relatively limited in the central region along the coaxial hole.

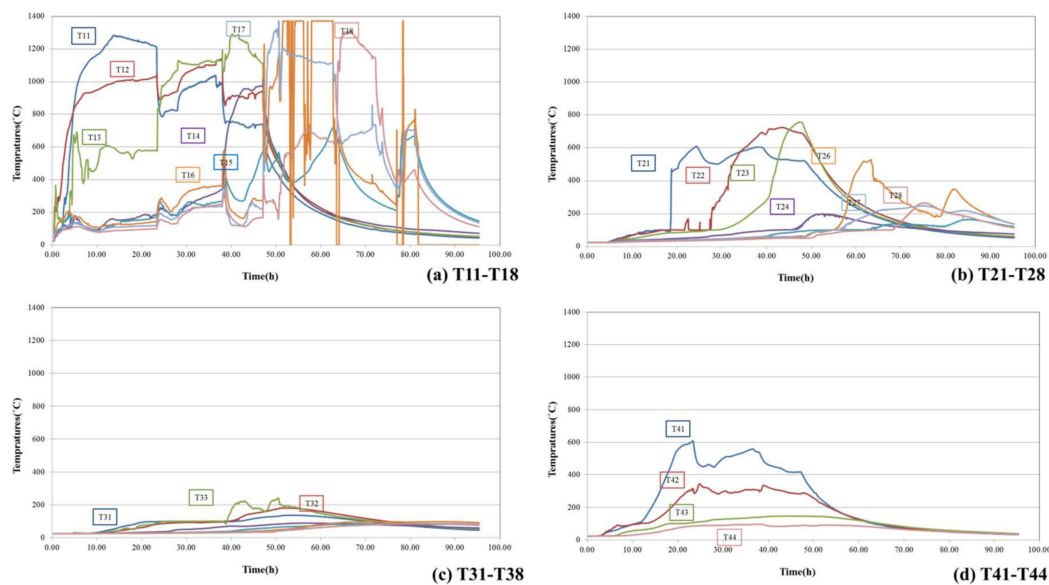


Figure 7. Temperature profiles during gasification experiment. (a) T11-T18; (b) T21-T28; (c) T31-T38; (d) T41-T44.

3.1.2. Gasification Zone Evolution

Based on the temperature data, two-dimensional maximum temperature profiles were plotted for several experimental periods in Figure 8a, representing the high temperature distribution in a cross-section of the horizontal well. Each figure shows results from a different position of an injection pipe. Additionally, the results of AE source locations are presented in Figure 8b. Using the onset time of AE waveforms recorded during UCG model experiments, AE source locations for each model were calculated using the least-squares iteration algorithm. The extent of damage, i.e., the relative energy emitted from cracking, can be indicated by the sphere sizes.

From the results in Figure 8a, the high temperature area moved when the injection position changed, meaning that the gasification area moved. This means that the gasification reactions are activated around an injection pipe. Gasification reactions are promoted under high temperature as a result of oxidation reactions. Therefore, the gasification area expanded around an injection pipe because most of the oxidant is consumed near the injection pipe. From a different perspective, it is possible to control the gasification area by changing the position of the injection agents. The results of AE source locations agree with those obtained from temperature profiles, meaning that many AE events occurred around the gasification area. Generation of these AEs apparently resulted from crack initiation and extension around the gasification area under the influence of thermal stress. Additionally, AE sources can be obtained in real-time during the UCG process. Accordingly, monitoring of AEs has been suggested to be an essential technique used to estimate damage zone development in real-time and inform operators when excessive damage occurs.

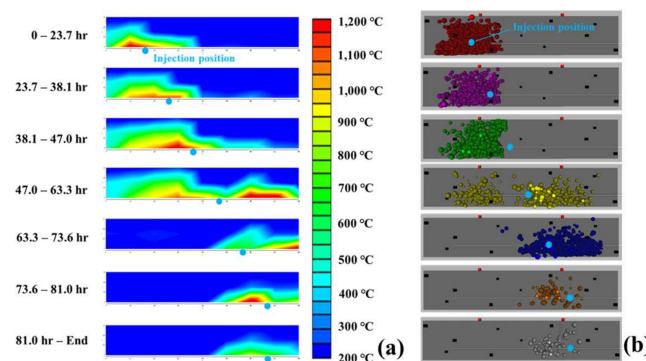


Figure 8. Comparison between results of temperature and AE monitoring. (a) Temperature distribution; (b) AE source location.

Figure 9 presents an estimation of the post-gasification cavity, based on a cross-section study every 100 mm. The cross-section consists of cavity, char, unreacted coal, and shale. Unfortunately, there is a shale seam in the upper part of the simulated coal seam because we obtained the simulated coal seam from an active open-cut coal mine in situ. From the results of Figure 9, the shape of the char-reflected gasification area agrees with the results of high temperature area distribution obtained from temperature profiles. Additionally, it can be said that a wide range of simulated coal seams are gasified in the lower part of the seam. This fact confirms the effectiveness of changing the position of the injection agents to expand the gasification area in the horizontal direction. The gasification area is limited around the middle part of the coal seam due to the effect of discontinuities caused by cementing concrete.

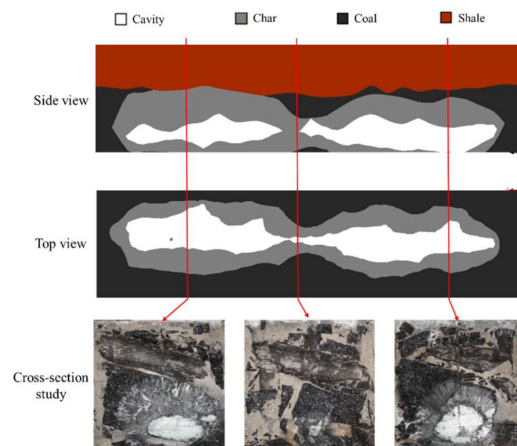


Figure 9. Estimation of post-gasification cavity.

3.2. Compositions of Product Gas and Calorific Value

Figure 10 shows the main compositions and calorific value of a product gas. There were no results from 38~47 h and 50~51 h elapsed due to problems with the monitoring system. The calorific value of the product gas could be calculated based on the combustible gas concentration, such as CO, H₂, CH₄, and other hydrocarbons [36].

During the initial period, CH₄ increased continuously and caused the first peak in calorific value (9.79 MJ/m³). The production of combustible gases such as CO, H₂, and CH₄ decreased slowly until the injection pipe was moved. The composition of the product gas dramatically changed and the calorific value reached a second peak (10.27 MJ/m³) when the position of the injection pipe was moved at approximately 23 h, meaning that combustible contents such as CO, H₂, CH₄ increased greatly and CO₂ decreased greatly. Latter stages also showed the same tendency: the calorific value reached a third peak (11.60 MJ/m³) at approximately 46 h and a fourth peak (9.73 MJ/m³) at 63 h. This fact showed the possibility to control the quality of the product gas by arranging the injection position of oxidants, although, slag formation usually inhibits the gasification reaction.

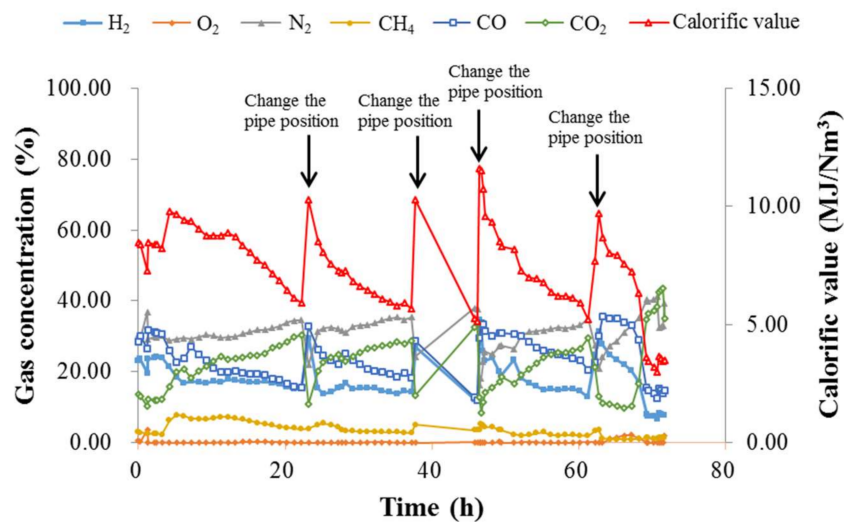


Figure 10. Main compositions and the calorific value of product gas.

3.3. Comparison with the Results of Previous Study

In order to evaluate the coaxial UCG system with a horizontal well, the comparison of results obtained from this study and a previous study [34] were conducted. Three types of model experiments were carried out in a previous study: coaxial 1 (injection ratio is 26 L/min and oxygen concentration is 58%), coaxial 2 (injection ratio is 20~50 L/min and oxygen concentration is 50%), and linking (injection ratio is 20~50 L/min and oxygen concentration is 58%), which is a conventional system. The experiments of coaxial 1 and 2 simulated the co-axial UCG system with a vertical well with length 400 mm. As a parameter to compare each UCG experiment, we calculated the gasification efficiency, i.e., the conversion efficiency of the consumed coal (chemical energy of product gas/chemical energy of consumed coal), as shown in Equation (1).

$$R_g = \frac{E_T/W_g}{Q_c}, \quad (1)$$

wherein R_g is the gasification efficiency (%), E_T means the total energy of product gas (MJ), W_g represents the consumed coal (kg), and Q_c stands for the coal calorific value (MJ/kg).

Total energy of product gas is calculated using the results of product gas composition and product gas flow rate. Additionally, the gasified coal is calculated based on balance computation of the C

element. Table 2 presents the calculation results for gasification efficiency. In the previous study, the values of gasification efficiency in coaxial 1 and 2, which simulate a coaxial UCG system, were 45.93% and 43.19%, respectively. By contrast, in linking, which aims to simulate a conventional UCG system, the gasification efficiency was 63.15%. From these results, it can be understood that a coaxial UCG system, with a vertical well, has lower efficiency for energy recovery from coal than that of a conventional UCG system, because of the low quality of product gas: 4.68 MJ/Nm³ for coaxial 1, 4.75 MJ/Nm³ for coaxial 2, and 7.78 MJ/Nm³ for linking. On the other hand, the results of the current study, about a coaxial system, demonstrate a gasification efficiency of 65.43%, producing a high quality of product gas (6.85 MJ/Nm³), meaning that the value is dramatically improved when compared with that of a conventional system. This finding suggests that the recovery energy of a coaxial UCG system can be improved with the control of the gasification area; by changing the outlet position of injection agents, the coaxial well can be prepared along coal seam dip.

Table 2. Calculation results of gasification efficiency.

| Linking-Hole Types | Co-Axial 1 | Co-Axial 2 | Linking-Hole | Co-Axial with a Horizontal Well |
|---|------------|------------|--------------|---------------------------------|
| Gasification period (hour) | 24 | 51 | 111 | 72 |
| Average calorific value (MJ/Nm ³) | 4.68 | 4.75 | 7.78 | 6.85 |
| Total energy (MJ) | 383.24 | 673.43 | 2804.82 | 1820.81 |
| Gasified coal (kg) | 25.91 | 48.54 | 138.28 | 86.63 |
| Gasification efficiency (%) | 45.93 | 43.19 | 63.15 | 65.43 |

4. Conclusions

Our research explored the coaxial UCG model by using an artificial coal seam, and the effective coal gasification in the coaxial UCG model was also observed. The initiation and extension of the gasification zone inside the coal could be visually monitored by the AE source locations. AE activity is closely related to local temperature change. Movement of the AE cloud also reflected the gasification area size and cavity growth in the gasifier. It could be confirmed that AE monitoring is available for evaluation of coal damage and gasification zone propagation during the gasification process.

This study focuses on the coaxial UCG system with a horizontal well; the injection position can be moved in order to improve the total efficiency of the gasification process. Results show that it is possible to control the gasification area by changing the position of the injection pipe; gasification reactions are activated around an injection pipe because most of the oxidant is consumed near the injection pipe.

Additionally, the recovered coal energy from a coaxial UCG system with a horizontal well is comparable with that of a conventional UCG system in terms of gasification efficiency, due to the large improvement in product gas quality. According to the experimental results, the average gas calorific value yielded in this coaxial model was 6.85 MJ/Nm³, which improved by approximately 30–50% compared when compared with small-scale laboratory tests conducted using the coaxial-hole model in our previous work. Therefore, a coaxial UCG system may be a feasible option to utilize coal resources abandoned underground, by controlling the injection position and designing a coaxial well along the coal seam dip.

Acknowledgments: This work was supported by the Japanese Society of UCG, Mikasa City, JSPS KAKENHI Grant Number 15H02332, Research Fund for the Doctoral Program of Higher Education of HPU (RFDP) Fund Number 660207/018, Scientific and technological research projects of Henan Province (182102310020 & 182102310889), Center of Environmental Science and Disaster Mitigation for Advanced Research of Muroran Institute of Technology and a Grant-in-Aid for Scientific Research (b), 21360441 from the Ministry of Education, Culture, Sports, Science, and Technology (MEXT), Japan. The authors gratefully acknowledge their support.

Author Contributions: Fa-qiang Su and Ken-ichi Itakura conceived and designed the experiments; Akihiro Hamanaka performed the experiments; Gota Deguchi carried out the gas analysis and analyzed the data; Wenyan Zhang and Hua Nan improved the language; Fa-qiang Su wrote the paper.

Conflicts of Interest: The authors declare no conflicts of interest.

References

1. Stańczyk, K.; Kapusta, K.; Wiatowski, M.; Swiadrowski, J.; Smoliński, A.; Rogut, J.; Kotyrba, A. Experimental simulation of hard coal underground gasification for hydrogen production. *Fuel* **2012**, *91*, 40–50. [\[CrossRef\]](#)
2. Shafirovich, E.; Varma, A. Underground coal gasification: A brief review of current status. *Ind. Eng. Chem. Res.* **2009**, *48*, 7865–7875. [\[CrossRef\]](#)
3. Alexander, Y.K. Early ideas in underground coal gasification and their evolution. *Energies* **2009**, *2*, 456–476.
4. Duan, T.; Wang, Z.; Liu, Z.; Chen, Y.; Fu, Z. Experimental Study of Coal Pyrolysis under the Simulated High-Temperature and High-Stress Conditions of Underground Coal Gasification. *Energy Fuels* **2017**, *31*, 1147–1158. [\[CrossRef\]](#)
5. Gregg, D.W.; Edgar, T.F. Underground coal gasification. *AIChE J.* **1978**, *24*, 753–781. [\[CrossRef\]](#)
6. Couch, G.R. *Underground Coal Gasification*; IEA Clean Coal Centre, International Energy Agency: London, UK, 2009.
7. Bhutto, A.W.; Bazmi, A.A.; Zahedi, G. Underground coal gasification: From fundamentals to applications. *Prog. Energy Combust. Sci.* **2013**, *39*, 189–214. [\[CrossRef\]](#)
8. Khan, M.M.; Mmbaga, J.P.; Shirazi, A.S.; Trivedi, J.; Liu, Q.; Gupta, R. Modelling Underground Coal Gasification—A Review. *Energies* **2015**, *8*, 12603–12668. [\[CrossRef\]](#)
9. Liu, S.; Zhang, S.; Chen, F.; Wang, C.; Liu, M. Variation of Coal Permeability under Dehydrating and Heating: A Case Study of Ulanqab Lignite for Underground Coal Gasification. *Energy Fuels* **2017**, *31*, 1147–1158. [\[CrossRef\]](#)
10. Khadse, A.; Qayyumi, P.; Mahajani, S.; Aghalayam, P. Underground coal gasification: A new clean coal utilization technique for India. *Energy* **2007**, *32*, 2061–2071. [\[CrossRef\]](#)
11. Bauman, J.H.; Deo, M. Simulation of a Conceptualized Combined Pyrolysis, In Situ Combustion, and CO₂ Storage Strategy for Fuel Production from Green River Oil Shale. *Energy Fuels* **2012**, *26*, 1731–1739. [\[CrossRef\]](#)
12. Prabu, V.; Jayanti, S. Heat-affected zone analysis of high ash coals during ex-situ experimental simulation of underground coal gasification. *Fuel* **2014**, *123*, 167–174. [\[CrossRef\]](#)
13. Nourozieh, H.; Kariznovi, M.; Chen, Z.; Abedi, J. Simulation Study of Underground Coal Gasification in Alberta Reservoirs: Geological Structure and Process Modeling. *Energy Fuels* **2010**, *24*, 3540–3550. [\[CrossRef\]](#)
14. Pei, P.; Barse, K.; Nasah, J. Competitiveness and Cost Sensitivity Study of Underground Coal Gasification Combined Cycle Using Lignite. *Energy Fuels* **2016**, *30*, 2111–2118. [\[CrossRef\]](#)
15. Burton, E.; Friedmann, J.; Upadhye, R. *Best Practices in Underground Coal Gasification*; Lawrence Livermore National Laboratory: Livermore, CA, USA, 2006.
16. Kacur, J.; Durdan, M.; Laciak, M.; Flegner, P. Impact analysis of the oxidant in the process of underground coal gasification. *Measurement* **2014**, *51*, 147–155. [\[CrossRef\]](#)
17. Nakaten, N.; Schlüter, R.; Azzam, R.; Kempka, T. Development of a techno-economic model for dynamic calculation of cost of electricity, energy demand and CO₂ emissions of an integrated UCG-CCS process. *Energy* **2014**, *66*, 779–790. [\[CrossRef\]](#)
18. Nakaten, N.C.; Kempka, T. Techno-Economic Comparison of Onshore and Offshore Underground Coal Gasification End-Product Competitiveness. *Energies* **2017**, *10*, 1643. [\[CrossRef\]](#)
19. Otto, C.; Kempka, T. Prediction of steam jacket dynamics and water balances in underground coal gasification. *Energies* **2017**, *10*, 739. [\[CrossRef\]](#)
20. Wang, Z.; Huang, W.; Zhang, P.; Xin, L. A contrast study on different gasifying agents of underground coal gasification at Huating Coal Mine. *J. Coal Sci. Eng. (China)* **2011**, *17*, 181–186. [\[CrossRef\]](#)
21. Kapusta, K.; Wiatowski, M.; Stańczyk, K. An experimental ex-situ study of the suitability of a high moisture ortho-lignite for underground coal gasification (UCG) process. *Fuel* **2016**, *179*, 150–155. [\[CrossRef\]](#)
22. Lin, X.; Liu, Q.; Liu, Z. Estimation of Effective Diffusion Coefficient of O₂ in Ash Layer in Underground Coal Gasification by Thermogravimetric Apparatus. *Energies* **2018**, *11*, 460. [\[CrossRef\]](#)
23. Imran, M.; Kumar, D.; Kumar, N.; Qayyum, A.; Saeed, A.; Bhatti, M.S. Environmental concerns of underground coal gasification. *Renew. Sustain. Energy Rev.* **2014**, *31*, 600–610. [\[CrossRef\]](#)

24. Otto, C.; Kempka, T. Thermo-Mechanical Simulations of Rock Behavior in Underground Coal Gasification Show Negligible Impact of Temperature-Dependent Parameters on Permeability Changes. *Energies* **2015**, *8*, 5800–5827. [[CrossRef](#)]
25. Kapusta, K.; Stańczyk, K. Pollution of water during underground coal gasification of hard coal and lignite. *Fuel* **2011**, *90*, 1927–1934. [[CrossRef](#)]
26. Kapusta, K.; Stańczyk, K.; Wiatowski, M.; Chečko, J. Environmental aspects of a field-scale underground coal gasification trial in a shallow coal seam at the Experimental Mine Barbara in Poland. *Fuel* **2013**, *113*, 196–208. [[CrossRef](#)]
27. Shu-qin, L.; Jing-gang, L.; Mei, M.; Dong-lin, D. Groundwater Pollution from Underground Coal Gasification. *J. China Univ. Min. Technol.* **2007**, *17*, 467–472.
28. Perkins, G.; Sahajwalla, V. A Numerical Study of the Effects of Operating Conditions and Coal Properties on Cavity Growth in Underground Coal Gasification. *Energy Fuels* **2006**, *20*, 596–608. [[CrossRef](#)]
29. Yong, C.; Jie, L.; Zhangqing, W.; Xiaochun, Z.; Chenzi, F.; Dongyu, L.; Xuan, W. Forward and reverse combustion gasification of coal with production of high-quality syngas in a simulated pilot system for in situ gasification. *Appl. Energy* **2014**, *131*, 9–19.
30. Itakura, K.; Goto, T.; Yoshida, K.; Belov, A.; Ram, G. Fundamental Experiments for Developing Underground Coal Gasification (UCG) System. *Mem. Muroran Inst. Technol.* **2010**, *59*, 51–54.
31. Hamanaka, A.; Su, F.Q.; Itakura, K.; Takahashi, K.; Kodama, J.; Deguchi, G. Effect of Injection Flow Rate on Product Gas Quality in Underground Coal Gasification (UCG) Based on Laboratory Scale Experiment: Development of Co-Axial UCG System. *Energies* **2017**, *10*, 238. [[CrossRef](#)]
32. Su, F.Q.; Itakura, K.; Deguchi, G.; Ohga, K. Monitoring of coal fracturing in underground coal gasification by acoustic emission techniques. *Appl. Energy* **2017**, *189*, 142–156. [[CrossRef](#)]
33. Su, F.Q.; Hamanaka, A.; Itakura, K.; Deguchi, G.; Satoh, K.; Kodama, J. Evaluation of Coal Combustion Zone and Gas Energy Recovery for Underground Coal Gasification (UCG) Process. *Energy Fuels* **2017**, *31*, 154–169. [[CrossRef](#)]
34. Hamanaka, A.; Itakura, K.; Su, F.Q.; Takahashi, K.; Satoh, K.; Deguchi, G.; Kodama, J. Model Experiment for Co-axial Underground Coal Gasification System Development. In Proceedings of the 24th World Mining Congress (Sustainability in Mining), Rio, Brazil, 18–21 October 2016; pp. 326–336.
35. Su, F.Q.; Nakanowataru, T.; Itakura, K.; Ohga, K.; Deguchi, G. Evaluation of Structural Changes in the Coal Specimen Heating Process and UCG Model Experiments for Developing Efficient UCG Systems. *Energies* **2013**, *6*, 2386–2406. [[CrossRef](#)]
36. Su, F.Q.; Itakura, K.; Deguchi, G.; Ohga, K.; Kaiho, M. Evaluation of energy recovery from laboratory experiments and small-scale field tests of underground coal gasification (UCG). *J. MMIJ* **2015**, *131*, 203–218. [[CrossRef](#)]

